

Supporting Information

Short two-armed lanthanide-binding tags for paramagnetic NMR spectroscopy based on chiral 1,4,7,10-tetrakis(2-hydroxypropyl)-1,4,7,10-tetraazacyclododecane scaffolds

Michael D. Lee,^a Matthew L. Dennis,^{a,b} Bim Graham^{*a} and James D. Swarbrick^{*a}

^aMonash Institute of Pharmaceutical Sciences, Monash University, Parkville VIC 3052, Australia. ^bCSIRO Biosciences Program, Parkville, VIC 3052, Australia.

E-mail: james.swarbrick@monash.edu; bim.graham@monash.edu

Contents

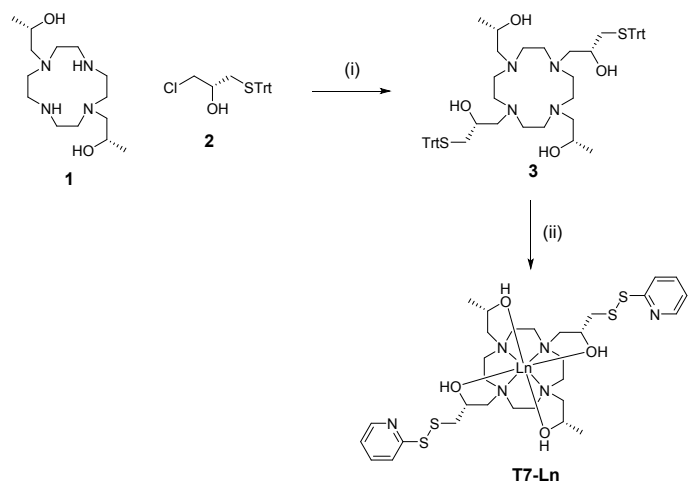
Materials and reagents.....	S2
Instruments.....	S2
Synthesis of T7 and metal complexes.....	S3
High-resolution mass spectrum of T7-Yb ³⁺	S5
¹ H and ¹³ C NMR spectra of novel compounds.....	S6
Ubiquitin and HPPK expression, purification and tagging.....	S8
Protein NMR spectroscopy and determination of $\Delta\chi$ and alignment tensors.....	S9
$\Delta\chi$ -Tensor parameters for T7 - and T8 -tagged ubiquitin E24C/A28C and T8 -tagged HPPK K76C/C80 (with metal ion coordinates and Euler angles).....	S10
Correlations between experimental and calculated PCSs for T7 - and T8 -tagged ubiquitin E24C/A28C and T8-tagged HPPK K76C/80C at pH 8.0.....	S11
¹⁵ N-HSQC spectra of T7 -tagged ubiquitin E24C/A28C at pH 6.5 and 8.0.....	S12
¹⁵ N-HSQC spectra of T8 -tagged ubiquitin E24C/A28C at pH 6.5 and 8.0.....	S13
¹⁵ N-HSQC spectra of T7 - and T8 -tagged HPPK K76C/C80	S14
Structures of ubiquitin and HPPK with Xplor-NIH modelled metal ion positions.....	S15
Correlations between PCSs measured with T7 - and T8 -tagged HPPK K76C/C80 loaded with Tm ³⁺	S16
Alignment tensor parameters for T8 -tagged ubiquitin E24C/A28C and HPPK K76C/C80.....	S17
Equation S1.....	S17
Correlations between experimental and calculated RDCs for T8 -tagged ubiquitin E24C/A28C and HPPK K76C/80C.....	S17
Orientations of the principal axes of the $\Delta\chi$ and alignment tensors.....	S18
Experimental PCSs measured for T7 - and T8 -tagged ubiquitin E24C/A28C and T7 - and T8 -tagged HPPK K76C/80C.....	S19
Experimental RDCs measured for T8 -tagged ubiquitin E24C/A28C and HPPK K76C/80C.....	S23
References.....	S24

Materials and reagents

(2S,2'S)-1,1'-(1,4,7,10-tetraazacyclododecane-1,7-diyl)bis(propan-2-ol)¹ (**1**) and (S)-1-chloro-3-(tritylthio)propan-2-ol (**2**)² were prepared following literature procedures. All other starting materials, reagents and solvents were obtained from commercial suppliers and were of general reagent or analytical grade and used without further purification.

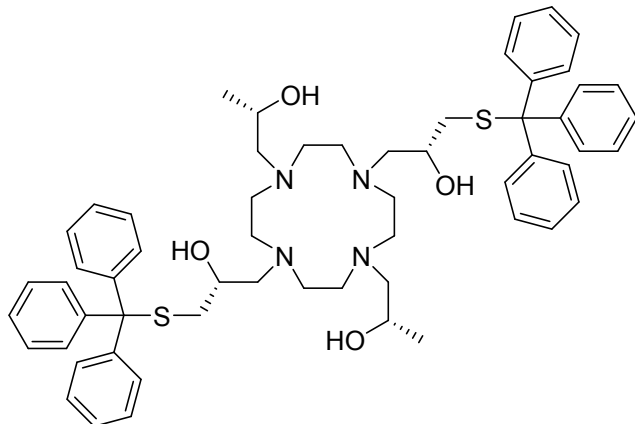
Instruments

All 400 MHz NMR spectra were recorded on a Bruker Avance III Nanobay spectrometer. NMR data was acquired using TOPSPIN/ICONNMR (Bruker), processing and plotting of the acquired data were performed using MestReNova software. Chemical shifts are quoted in units of parts per million (ppm) and were referenced internally to the residual proteo-solvent resonance; ¹H NMR: CDCl₃ (δ 7.26), D₂O (δ 4.79); ¹³C NMR: CDCl₃ (δ 77.16).³ Multiplicity for NMR resonances are abbreviated as; s, singlet; d, doublet; t, triplet; q, quartet; p, pentet; m, multiplet, app, apparent; br, broad. LCMS were acquired on an Agilent 1220/6120 LCMS system, using ChemStation software for instrument control and data analysis. HRMS were acquired on an Agilent 6224 TOF LCMS mass spectrometer, coupled to an Agilent 1290 Infinity (Agilent, Palo Alto, CA). Acquisition was performed using Agilent Mass Hunter Data Acquisition software and analyzed using Mass Hunter Qualitative Analysis software. Preparative reverse-phase HPLC was performed on an Agilent 1260 Prep HPLC using an Alltima C8 column (250 mm x 22 mm, 5 micron).



Scheme S1. Synthesis of lanthanide complexes of **T7**. Reagents and conditions: (i) K_2CO_3 , ACN, reflux, 72 h, 58%; (ii) LnCl_3 , MeOH, reflux, 2 h, 2,2'-pyridyldisulfide, silver nitrate, RT, 2 h, 14%.

(2*R*,2*'R*)-3,3'-(4,10-bis((*S*)-2-Hydroxypropyl)-1,4,7,10-tetraazacyclododecane-1,7-diyl)bis(1-tritylthio)propan-2-ol, **3**



K_2CO_3 (262 mg, 1.90 mmol) was added to a solution of **1** (110 mg, 0.38 mmol) and **2** (350 mg, 0.95 mmol) in ACN (6 mL) and heated to reflux for 24 h, after which additional **5** (350mg, 0.95 mmol) was added and reflux continued for a further 48 h. After cooling to room temperature, insoluble salts were removed by filtration and the filtrate concentrated under reduced pressure. The resulting crude residue was purified by silica flash chromatography (0 to 5% MeOH and 0.5% NH_3 in CHCl_3) to yield **6** as an off-white foam. Yield: 212 mg (58%). **¹H NMR** (400 MHz, CDCl_3) δ 7.42 (m, 12 H), 7.27 (m, 12H), 7.19 (m, 6H), 5.33 (br, 2H), 4.80 (br, 2H), 3.78 (br, 2H), 3.41 (br, 2H), 2.79 (m, 7H), 2.46 (m,

3H), 2.17 (m, 8H), 1.98 (m, 8H), 1.05 (m, 6H). **¹³C NMR** (100 MHz, CDCl₃) δ 144.97 (C), 129.80 (CH), 128.06 (CH), 126.77 (CH), 66.87 (C(Ph)₃), 66.00 (CH), 62.70 (CH), 62.53, 60.06, 52.63, 49.94, 37.79 (previous 5 peaks CH₂), 22.40 (CH₃). **HRMS** (ESI) *m/z* calcd [M+H]⁺ C₅₈H₇₃N₄O₄S₂: 953.5073, found: 953.5084.

Formation of metal complexes

A solution of **3** (15 mg, 0.016 mmol) and YCl₃(H₂O)₆ (7 mg, 0.024 mmol) in MeOH (2 mL) was heated at 60 °C for 2 h. After cooling to room temperature, silver nitrate (27 mg, 0.16 mmol) and 2,2'-dipyridyldisulfide (21 mg, 0.096 mmol) were added and the mixture stirred vigorously for 2 h at room temperature, during which time a cloudy beige precipitate that gradually turned grey formed. Insoluble material was sedimented by transferring the reaction mixture to a 15 mL centrifuge tube and centrifugation at 2000 rcf for 5 min. The supernatant was removed and syringe filtered through a 45 μm membrane, before concentration under reduced pressure. The resulting residue was purified by reverse-phase HPLC (0.1 % TFA and a 5–100% ACN gradient over 30 min on a C8 preparative column). Fractions containing pure product were lyophilised to afford **T7-Y³⁺** as a white solid. Yield: 3 mg (14 %, based on a pentatrifluoroacetate salt). **¹H NMR** (400 MHz, D₂O) δ 8.52 (dd, *J* = 5.3, 0.9 Hz, 2H), 8.06 (m, 2H), 7.98 (d, *J* = 8.2 Hz, 2H), 7.51 (ddd, *J* = 7.4, 5.3, 1.1 Hz, 2H), 4.65 (m, 2H), 4.57 (m, 2H), 3.50 (m, 6H), 3.32 (m, 4H), 3.17 (m, 2H), 3.06–2.91 (m, 4H), 2.77 (dd, *J* = 12.9, 4.1 Hz, 2H), 2.52–2.31 (m, 8H), 2.26 (br d, *J* = 13.8 Hz, 2H), 1.27 (d, *J* = 5.9 Hz, 6H). **HRMS** (ESI) *m/z* calcd [M+H]⁺ C₃₀H₄₈N₆O₄S₄Y: 773.1673 , found 773.1687.

The Tm³⁺ and Yb³⁺ complexes of **T7** were formed in an analogous manner to the Y³⁺ complexes. **T8** and its lanthanide complexes were synthesised following the same methods used to synthesise **T7**, with the replacement of (*S*)-propylene oxide and (*S*)-epichlorohydrin (for the synthesis of **1** and **3**) with their commercially available enantiomers. **HRMS** and **¹H NMR** of the Yb³⁺ complexes of **T7** are shown in **Figures S1 and S3**.

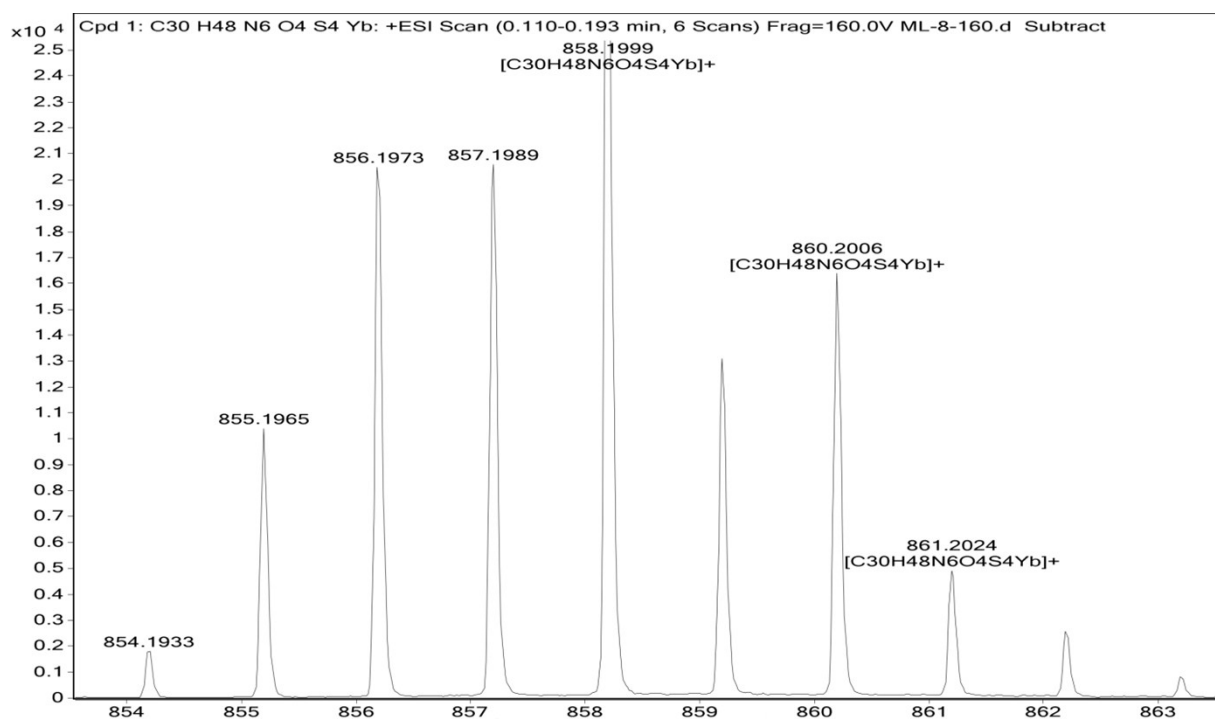


Figure S1. High-resolution mass spectrum of T7-Yb^{3+} .

Table S1. Predicted masses of T7-Yb^{3+} .

Complex	Chemical formula	Predicted masses (relative abundance) ^a
T7-Yb^{3+}	$[\text{C}_{30}\text{H}_{48}\text{N}_6\text{O}_4\text{S}_4\text{Yb}]^+$	858.2003 (100.0%), 856.1979 (68.6%), 857.1997 (50.7%), 855.1978 (44.9%), 860.2041 (40.1%), 859.2037 (32.4%), 857.2012 (22.3%), 860.1961 (18.1%), 858.2030 (16.4%), 856.2012 (14.6%).

^aOnly masses of the 10 highest abundance predicted species are listed.

Figure S2. 1D ^1H NMR and ^{13}C NMR spectra of **3**.

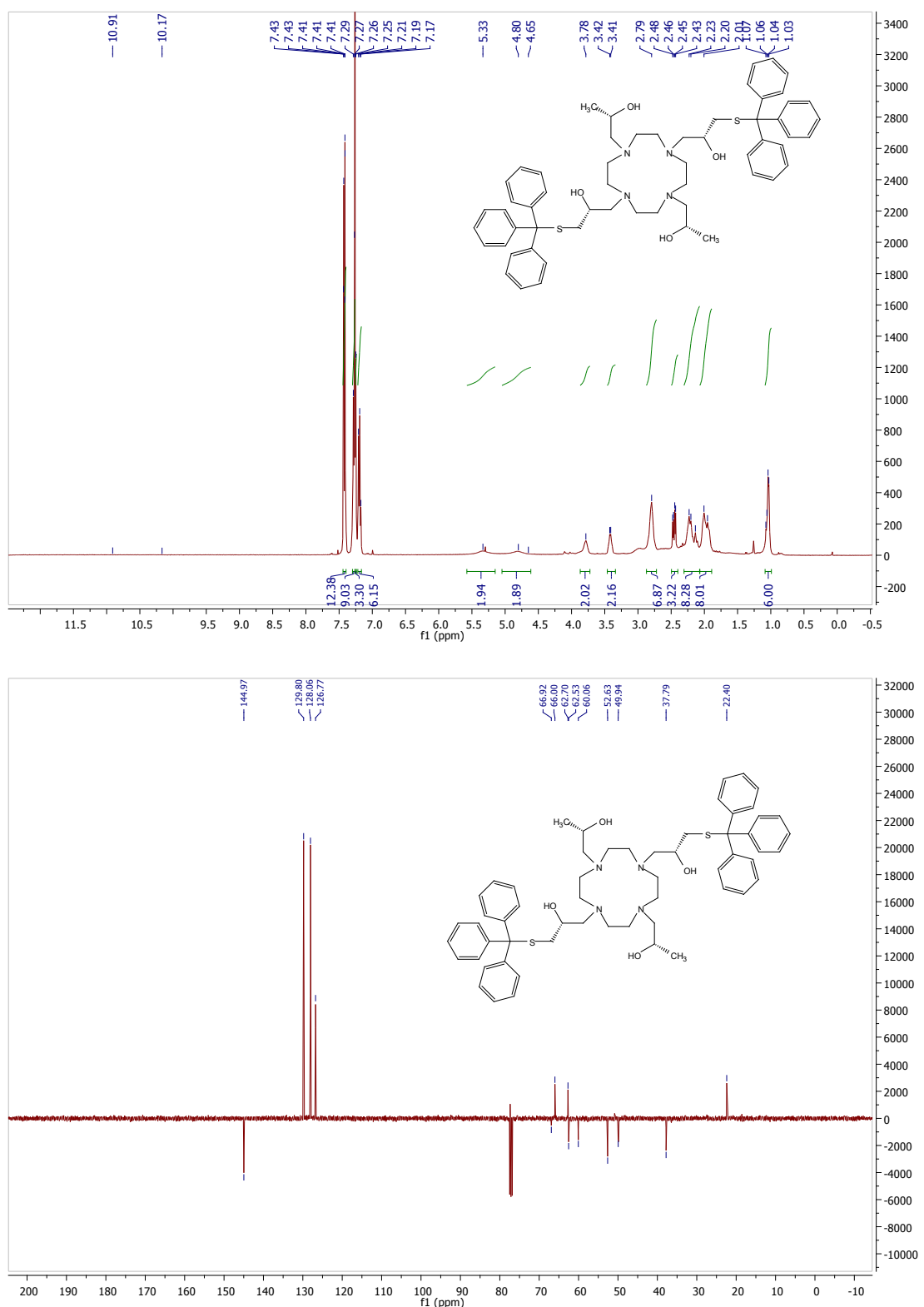
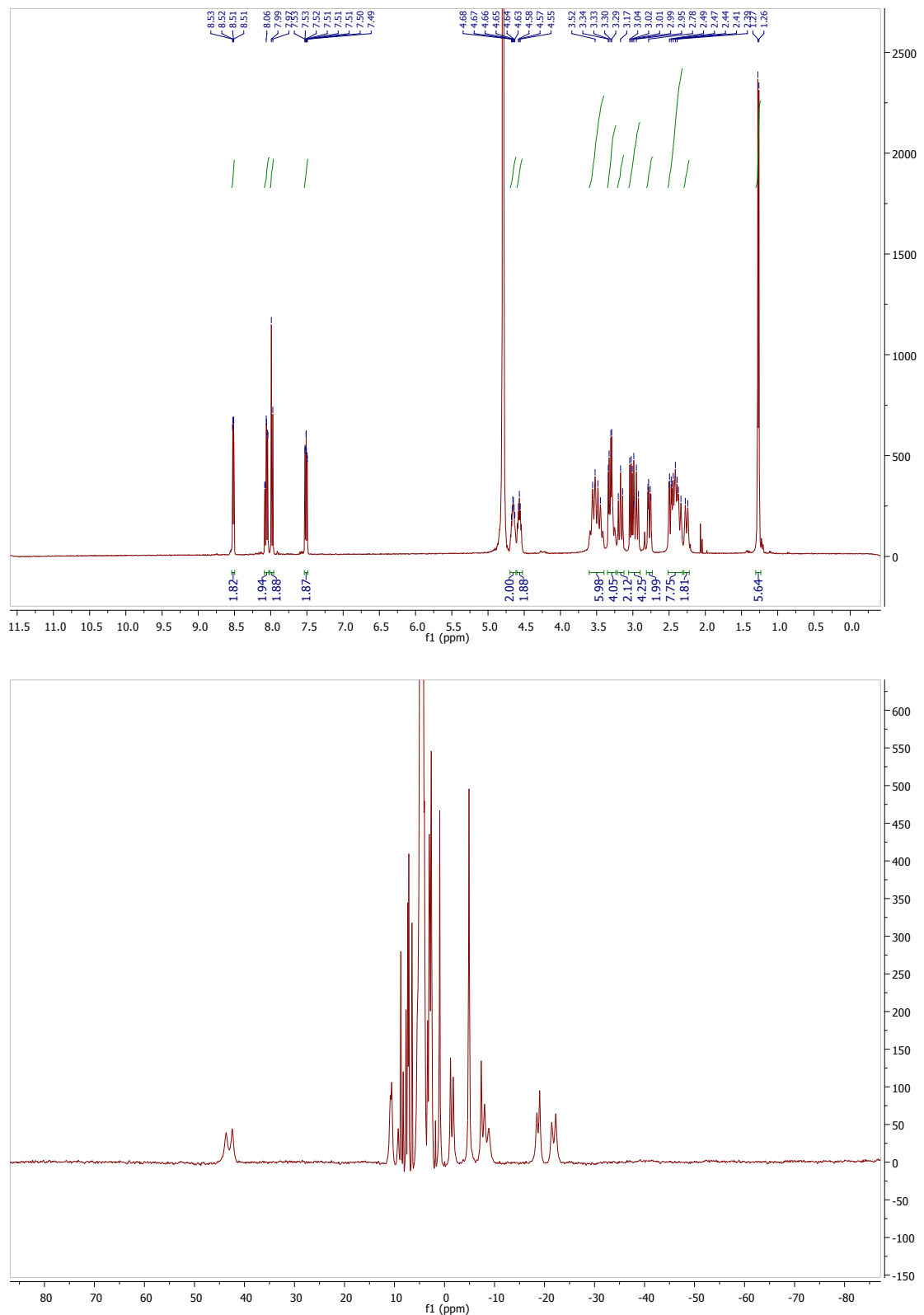


Figure S3. 1D ^1H NMR spectra of Y^{3+} (upper) and Yb^{3+} (lower) complexes of **T7**.



Ubiquitin E24C/A28C expression, purification and tagging

Uniformly ^{15}N -labelled ubiquitin E24C/A28C prepared as described.⁴ The protein was first reduced by stirring with 20 equivalents of DTT for 1 h at room temperature. The protein was then passed through a PD 10 column equilibrated with degassed buffer (50 mM HEPES, pH 8.0). Five equivalents of **T7** or **T8** loaded with Tm^{3+} , Yb^{3+} or Y^{3+} were diluted in 300 μL of buffer and added to the protein, and the solutions stirred over ice for 1 h. Excess tag was removed by passage through a PD10 column equilibrated with either 50 mM HEPES, pH 8.0, or 50 mM MES, pH 6.5 and the eluate concentrated in an Amicon ultrafiltration centrifugal tube with a molecular weight cut-off of 3 kDa, to a final protein concentration of approximately 100 μM . Prior to NMR measurements, each sample was made to 10% D_2O (v/v).

HPPK K76C/C80 expression, purification and tagging

The HPPK 76C/C80 mutant gene cloned into a pET28a vector was purchased from Geneart.

Uniformly ^{15}N -labelled HPPK 76C/C80 was expressed and purified following established protocols for the wild-type protein.⁵

Purified, uniformly ^{15}N -labelled HPPK K76C/C80 was passed through a PD10 column equilibrated with degassed buffer (50 mM HEPES, pH 8.0) to remove DTT present in the storage buffer. The eluate was then made to 10 mM magnesium chloride and 100 μM α,β -methyleneadenosine 5'-triphosphate. Three equivalents of **T8** loaded with Tm^{3+} , Yb^{3+} or Y^{3+} were diluted in 300 μL of buffer and added to the protein, and the solutions stirred over ice for 15 min. Excess tag was removed by passage through a PD10 column (50 mM HEPES, pH 8.0). The eluate was again made to 10 mM magnesium chloride and 100 μM α,β -methyleneadenosine 5'-triphosphate, before concentrating in an Amicon ultrafiltration centrifugal tube with a molecular weight cutoff of 3 kDa, to a final protein concentration of approximately 100 μM . Prior to NMR measurements, the samples were made to 1 mM α,β -methyleneadenosine 5'-triphosphate and 400 μM of 8-mercaptoguanine (a small molecule HPPK inhibitor) and the sample adjusted to 10% D_2O (v/v).

Protein NMR spectroscopy and $\Delta\chi$ -tensor and alignment tensor determination

Spectra of differently tagged ubiquitin E24C/A28C and HPPK K76C/C80 samples were recorded at 25 °C and 22 °C, respectively, on a Bruker Avance 600 MHz NMR spectrometer equipped with a cryogenic probe and Z axis gradient. $^1\text{H}^{\text{N}}$ PCSs and $^1D_{\text{HN}}$ couplings were measured by recording ^{15}N -fast-HSQC and IPAP-[^{15}N , ^1H]-HSQC spectra. Data were processed with NMRPipe⁶ and analyzed with SPARKY.⁷

Calculation of $\Delta\chi$ -tensors was carried out within the program Numbat.⁸ The $\Delta\chi$ -tensors were fitted to the first conformer of the NMR structure of ubiquitin (PDB 2MJB⁹) or the X-ray crystal structure of HPPK (PDB 3QBC⁵). Unambiguous PCS assignments were used to calculate an initial estimate of the $\Delta\chi$ -tensor, which was used to predict PCSs of other nuclei to assist the assignment of further PCSs and refine the $\Delta\chi$ -tensors in an iterative manner. The measured PCSs are listed in **Tables S4 and S5**.

Backbone amide $^1D_{\text{HN}}$ RDCs were fitted to the first conformer of the NMR structure of ubiquitin (PDB 2MJB⁹) or the X-ray crystal structure of HPPK (PDB 3QBC⁵) using single value decomposition *via* the “-bestFit” flag in PALES.¹⁰ The measured RDCs are listed in **Tables S6**.

Table S2. $\Delta\chi$ -Tensor parameters for T7- and T8-conjugated ubiquitin E24C/A28C and HPPK K76C/C80 ^a														
Protein	Tag	pH	Ln ³⁺	# PCS	$\Delta\chi_{\text{ax}}$	$\Delta\chi_{\text{rh}}$	Q	x	y	z	α	β	γ	
Ubiq	T7	8.0	Tm ³⁺	36	45.0 (0.9)	18.7 (0.6)	0.01	4.057	2.980	-11.759	84	130	107	
			Yb ³⁺	41	-11.8 (0.2)	-4.1 (0.2)	0.06	4.057	2.980	-11.759	38	40	106	
	6.5		Tm ³⁺	46	47.1 (0.4)	18.6 (0.4)	0.02	4.143	3.504	-11.760	84	127	110	
			Yb ³⁺	50	-12.1 (0.1)	-6.4 (0.2)	0.04	4.143	3.504	-11.760	31	37	116	
Ubiq	T8	8.0	Tm ³⁺	28	-39.9 (1.6)	-21.0 (0.9)	0.01	2.798	3.560	-11.628	61	65	83	
			Yb ³⁺	37	13.7 (0.7)	6.8 (0.4)	0.04	2.798	3.560	-11.628	137	100	155	
	6.5		Tm ³⁺	32	44.0 (1.0)	11.8 (1.7)	0.01	4.092	1.618	-12.434	23	156	76	
			Yb ³⁺	37	-6.8 (0.4)	-2.3 (0.2)	0.06	4.092	1.618	-12.434	32	78	110	
HPPK	T7	8.0	Tm ³⁺	36	47.4 (0.3)	19.9 (0.5)	0.02	-16.439	11.961	2.542	150	101	179	
HPPK	T8	8.0	Tm ³⁺	102	57.8 (1.1)	15.3 (0.7)	0.04	-16.639	11.227	3.567	131	147	164	
			Yb ³⁺	108	-9.0 (0.2)	-2.8 (0.1)	0.06	-16.639	11.227	3.567	54	83	116	

^a The axial and rhombic components of the $\Delta\chi$ -tensors are reported in units of 10^{-32} m^3 , and the Euler angles in degrees, using the xyz convention and unique tensor representation.⁸ Standard deviations (in brackets) were determined from random removal of 10% of the PCSSs and recalculating the $\Delta\chi$ -tensors 1,000 times. Quality factors (Q) were calculated as the root-mean-square deviation between the experimental and back-calculated PCSSs divided by the root-mean-square of the experimental PCSSs. Metal coordinates (x, y, z) are reported relative to the NMR structure of ubiquitin (PDB ID 2MJB⁹) or the X-ray crystal structure of HPPK (PDB 3QBC⁵).

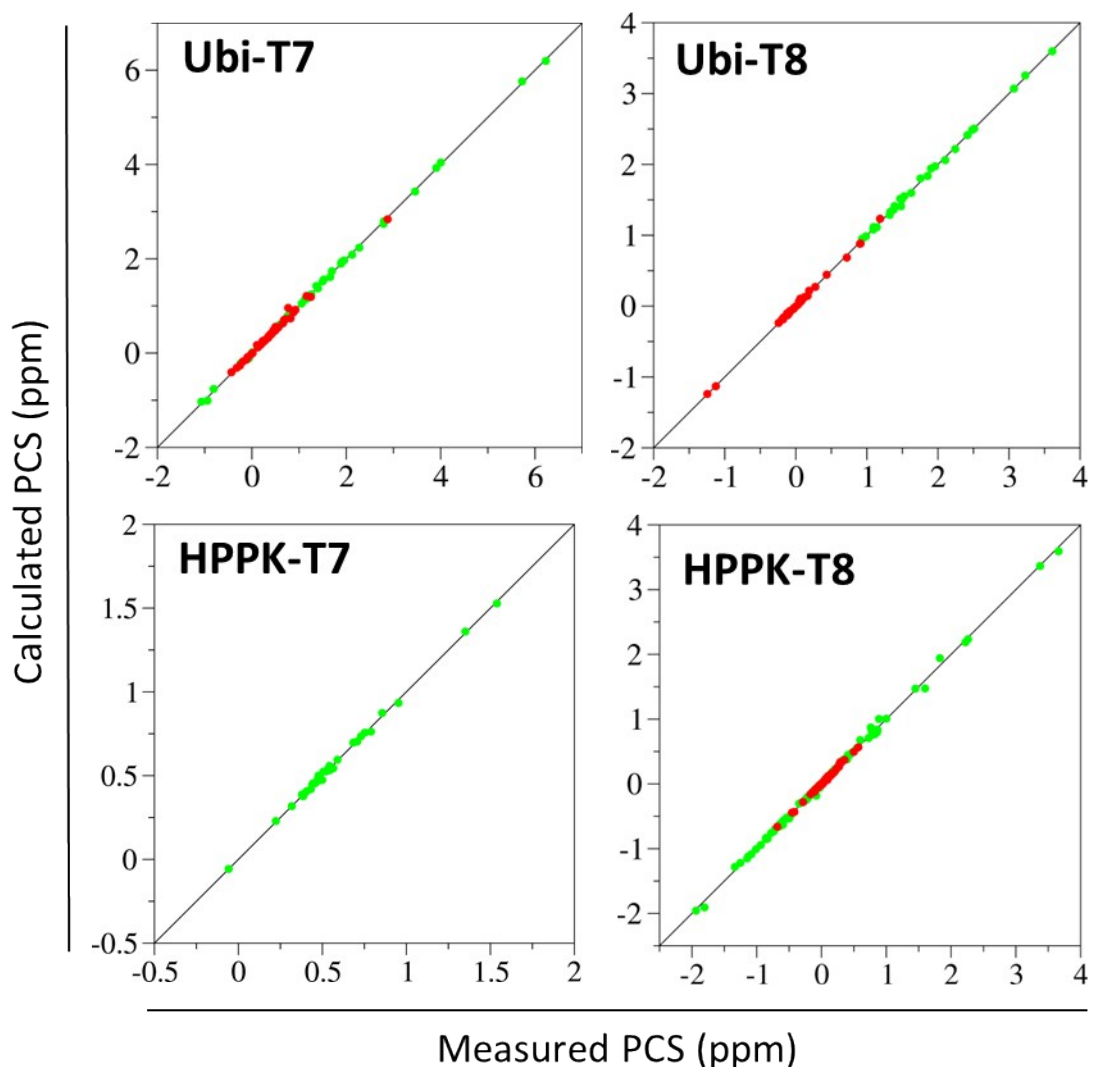


Figure S4. Correlations between experimental and calculated PCSs for **T7**- and **T8**-tagged ubiquitin E24C/A28C and HPPK S112C/C80A, loaded with Tm³⁺ (green) or Yb³⁺ (red). Solid lines represent perfect correlation.

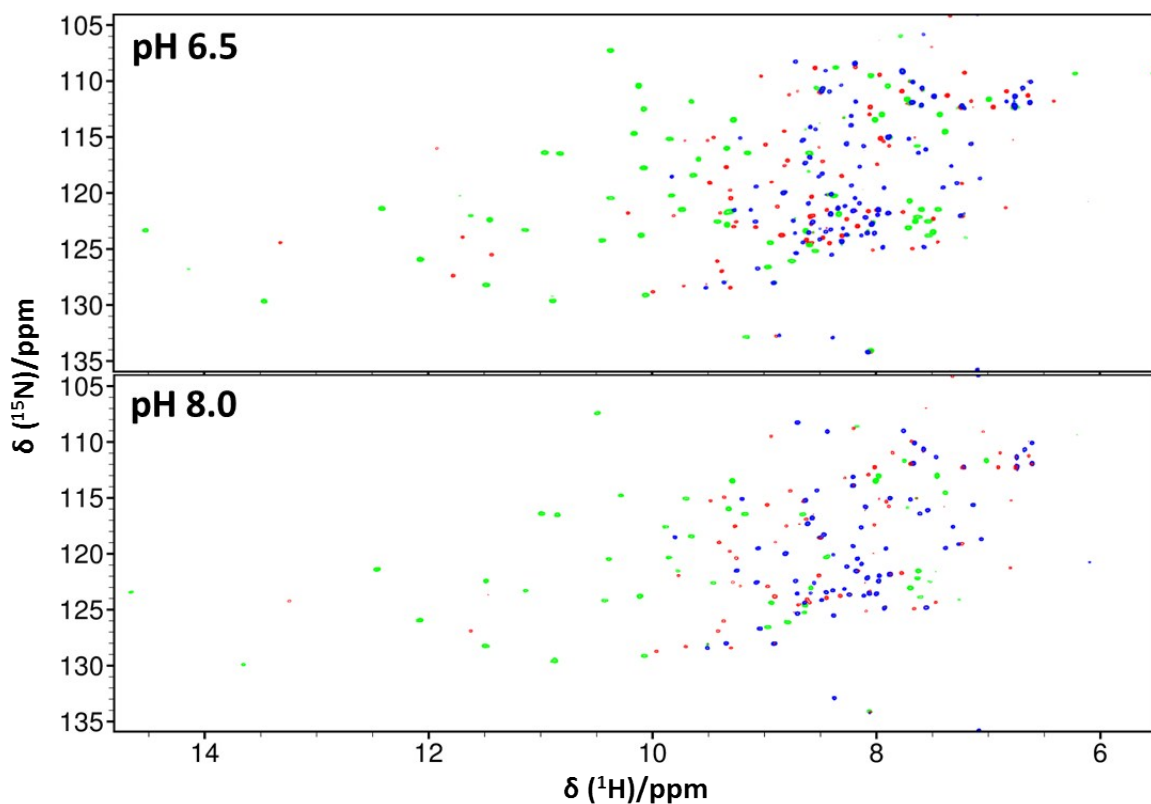


Figure S5. Overlays of ^{15}N -HSQC spectra of T7-tagged ubiquitin E24C/A28C, loaded with either Y^{3+} (blue), Tm^{3+} (green) or Yb^{3+} (red). The spectra were recorded at 25 °C and pH 6.5 (top) or pH 8.0 (bottom), at a ^1H NMR frequency of 600 MHz.

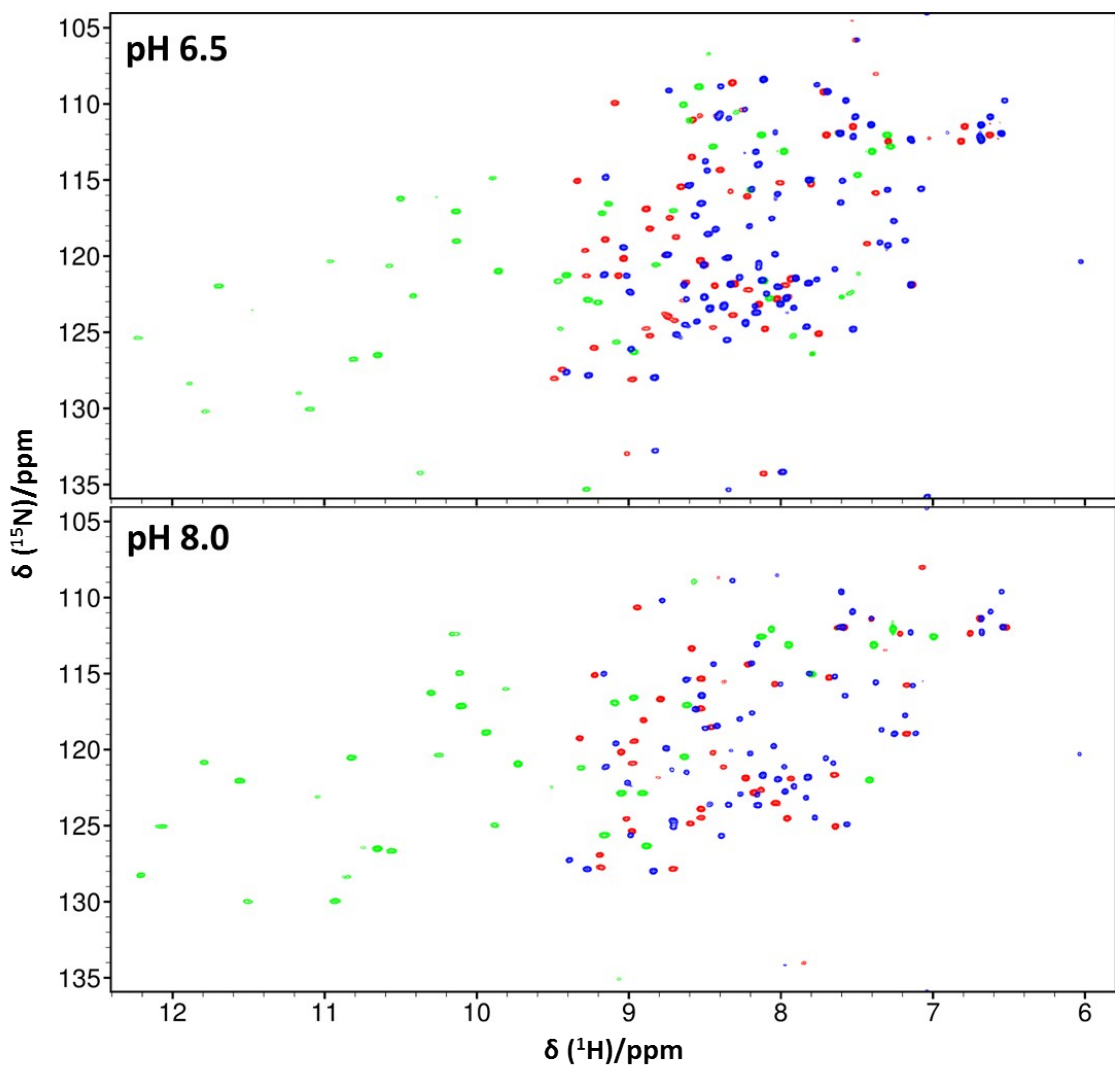


Figure S6. Overlays of ^{15}N -HSQC spectra of **T8**-tagged ubiquitin E24C/A28C, loaded with either Y^{3+} (blue), Tm^{3+} (green) or Yb^{3+} (red). The spectra were recorded at 25 °C and pH 6.5 (top) or pH 8.0 (bottom), at a ^1H NMR frequency of 600 MHz.

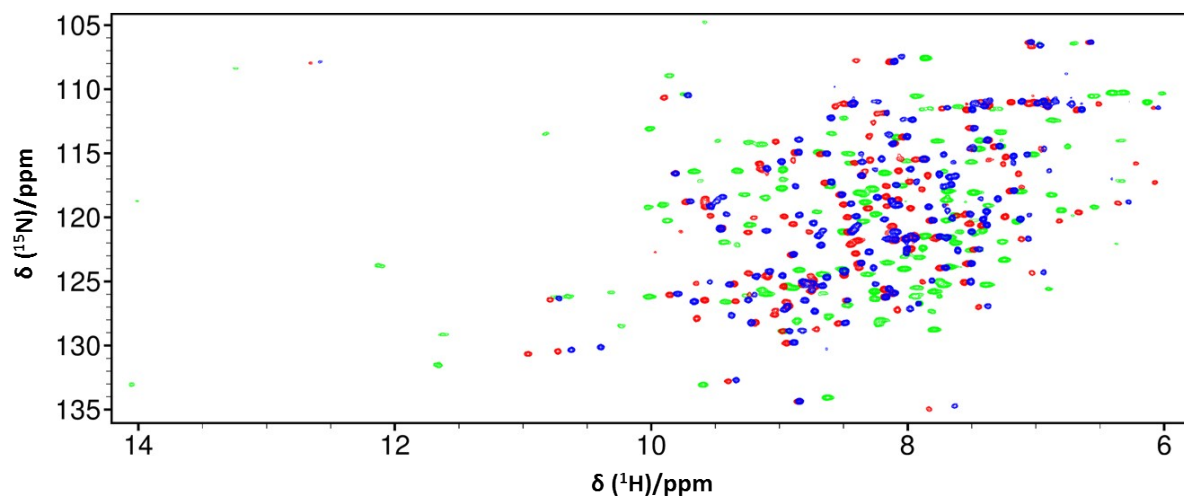


Figure S7. Overlays of ^{15}N -HSQC spectra of T8-tagged HPPK K76C/C80, loaded with either Y^{3+} (blue), Tm^{3+} (green) or Yb^{3+} (red). The spectra were recorded at 22 °C and pH 8.0 at a ^1H NMR frequency of 600 MHz, in the presence of 10 mM MgCl_2 , 1 mM α,β -methyleneadenosine 5'-trisphosphate and 400 μM of a small-molecule inhibitor, 8-mercaptoguanine.

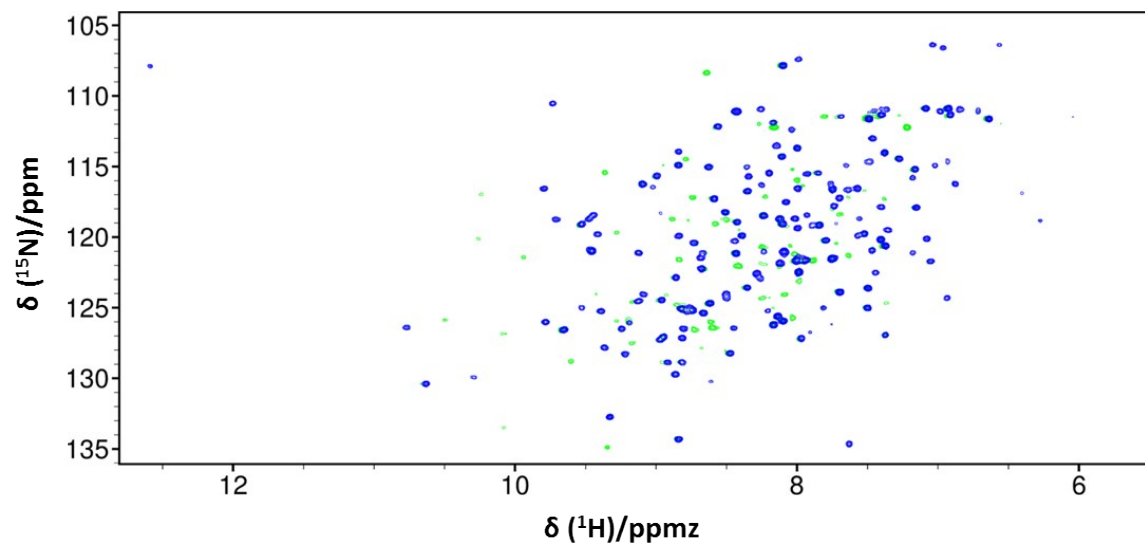


Figure S8. Overlays of ^{15}N -HSQC spectra of T7-tagged HPPK K76C/C80, loaded with either Y^{3+} (blue) or Tm^{3+} (green). The spectra were recorded at 22 °C and pH 8.0 at a ^1H NMR frequency of 600 MHz, in the presence of 10 mM MgCl_2 , 1 mM α,β -methyleneadenosine 5'-trisphosphate and 400 μM of a small-molecule inhibitor, 8-mercaptoguanine.

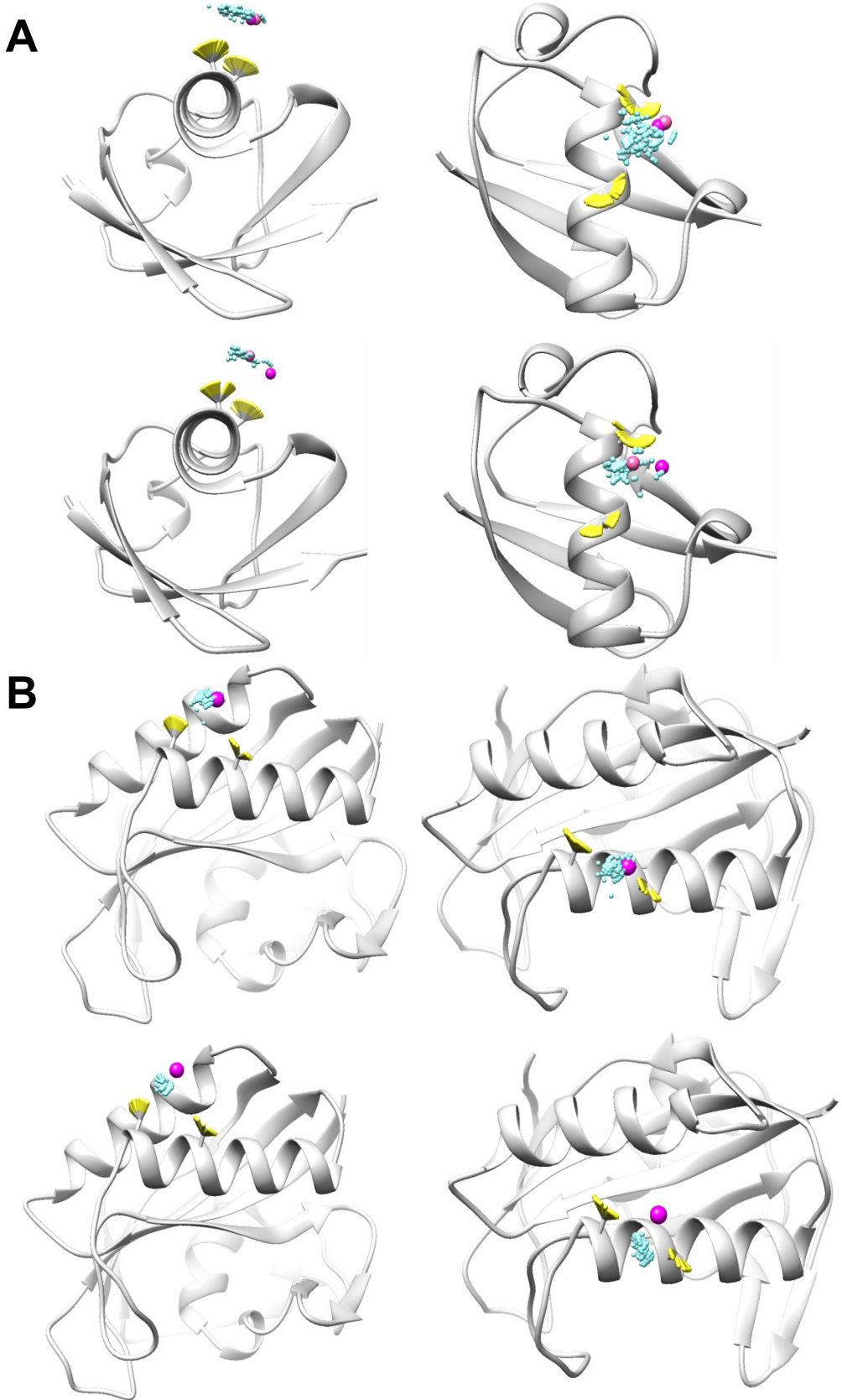


Figure S9. Modelled and PCS-determined metal ion positions. Cloud of 400 metal positions (cyan) as modelled in Xplor-NIH. A) T7 (top) and T8 (bottom) attached to ubiquitin. The larger spheres are the PCS determined common metal ion position (for each tag loaded with either Yb^{3+} or Tm^{3+}) and recorded at pH 8 (magenta) and pH 6.5 (pink) respectively. The sidechains of Cys24 and Cys28 are shown in yellow. B) T8 (top) and T7 (bottom) attached to HPPK showing the PCS determined metal position (magenta) and the sidechains of Cys76 and Cys80 shown in yellow.

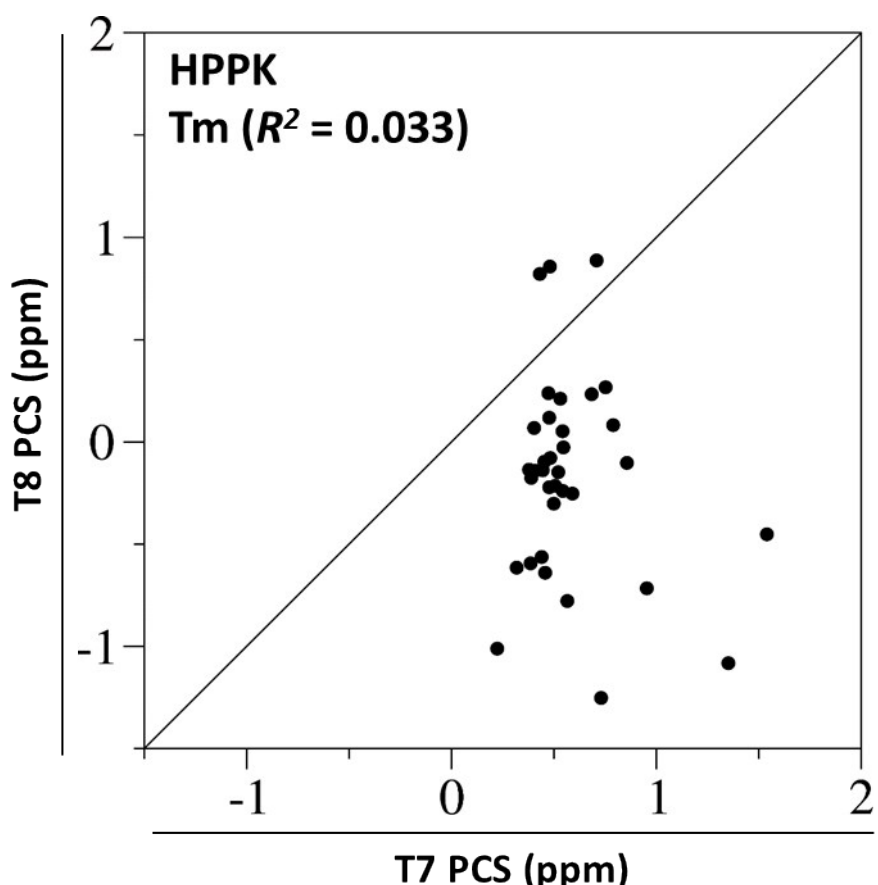


Figure S10. Correlations between PCSs measured with T7- and T8-tagged HPPK K76C/C80 loaded with Tm³⁺. Only PCSs that were measured with both tags are shown. The solid line represents perfect correlation.

Table S3 Alignment tensor parameters for **T8-Tm³⁺**-tagged ubiquitin E24C/A28C and HPPK K76C/C80^a

Protein	Tag	# RDC	A _{ax}	A _{rh}	Q	α	β	γ	Δχ _{ax} ^b	Δχ _{rh} ^b
Ubi	T8-Tm ³⁺	24	-9.8	-3.2	0.23	107	69	111	-38.2	-12.5
HPPK	T8-Tm ³⁺	66	13.3	2.8	0.12	13	146	53	51.3	10.8

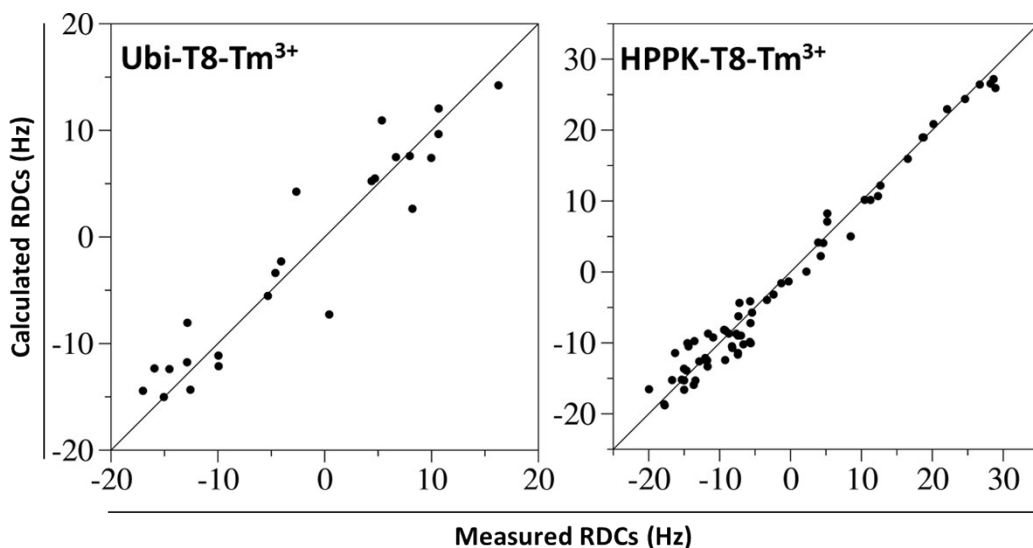
^aThe axial and rhombic components of the alignment tensor are reported in units of 10⁻⁴ and the Euler angles in degrees, using the *xyz* convention, values were determined by fitting the measured RDCs to the NMR structure of ubiquitin (PDB ID 2MJB⁹) or the X-ray crystal structure of HPPK (PDB ID 3QBC⁵) respectively, using the “–bestFit” flag within PALES.¹⁰ Quality factors (*Q*) were calculated as the root-mean-square deviation between the experimental and back-calculated RDCs divided by the root-mean-square of the experimental RDCs.

^bΔχ-Tensor parameters in units of 10⁻³² m³ determined from the A_{ax} and A_{rh} using Equation S1.

Equation S1. For comparison of A_{ax,rh} and Δγ_{ax,rh}

$$\Delta\chi_{ax,rh} = A_{ax,rh} \frac{15\mu_0 KT}{B_0^2}$$

where B₀ is the field strength (14.1 T), μ₀ is the magnetic permeability of vacuum (12.566 × 10⁻⁷ T² m³ J⁻¹), *k* is the Boltzmann constant (1.38 × 10⁻²³ J K⁻¹), *T* is temperature (in Kelvin), Δχ_{ax,rh} are the axial and rhombic components of the magnetic susceptibility anisotropy tensor (in m³) respectively and A_{ax,rh} are the axial and rhombic components of the alignment tensor respectively.

**Figure S11.** Correlations between experimental and calculated ¹D_{HN} RDCs recorded at a ¹H NMR frequency of 600 MHz and pH 8.0 for **T8-Tm³⁺**-tagged ubiquitin E24C/A28C (left) and HPPK K76C/C80A (right). Solid lines represent perfect correlation.

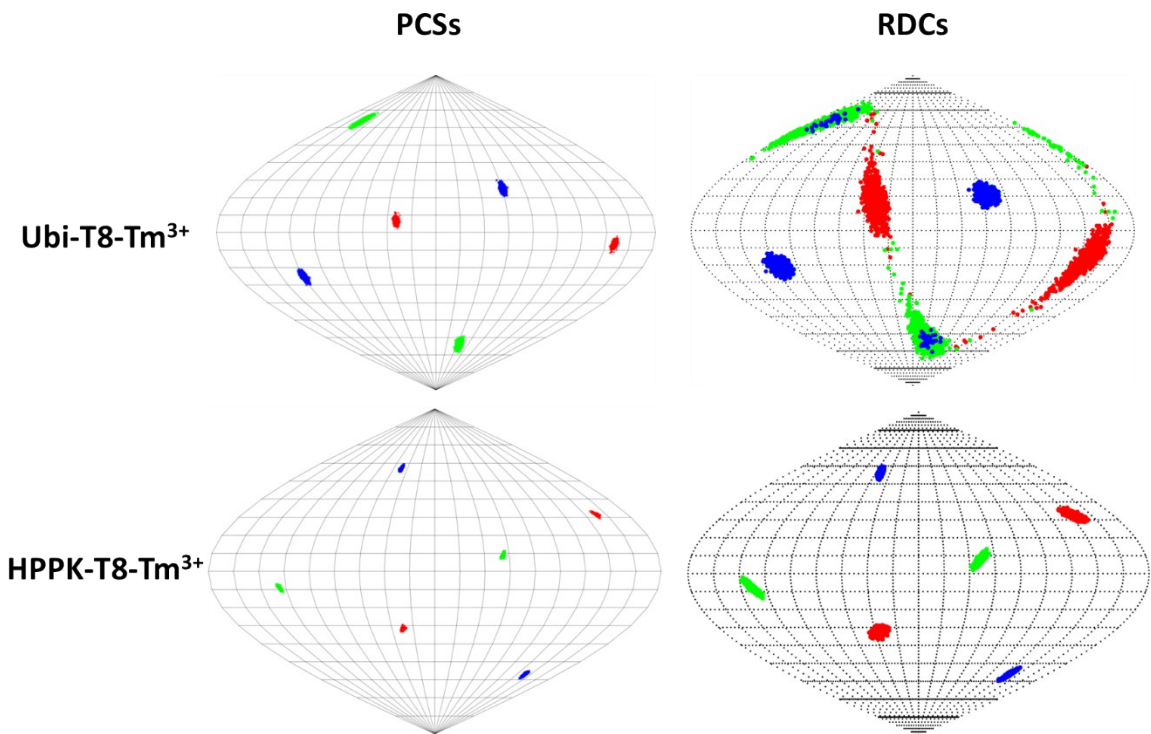


Figure S12. Orientations of the principal axes of the $\Delta\chi$ - (left) and alignment (right) tensors. The points show where the principal axes of the tensors penetrate the sphere with the axes colored as follows: z (blue), y (green), x (red). For the $\Delta\chi$ -tensors, 1000 replicates with a random 10% of the PCS data removed each time are shown. For the alignment tensors, 1000 replicates of SVD calculation using the structural noise Monte-Carlo method ('-mcStruc') within PALES¹⁰ are shown.

Table S4. Experimental PCSs (ppm) for tagged ubiquitin E24C/A28C.

Residue	pH 8.0				pH 6.5			
	T7		T8		T7		T8	
	Tm ³⁺	Yb ³⁺						
2 GLN	1.96	0.34	0.93	0.11	1.90	0.39	1.15	0.19
3 ILE	2.79	0.56	1.63	0.03	2.74	0.60	2.11	0.25
4 PHE	1.91	0.42	1.76	-0.03	1.86	0.42	2.09	0.21
5 VAL	1.89	0.53	1.90	-0.17	1.87	0.54	2.32	0.12
6 LYS	1.17	0.40	2.10	-0.12	1.14	0.39	2.27	0.14
7 THR	0.68	0.35	1.48	-0.10	0.68	0.34	1.53	0.05
8 LEU					0.21	0.27	1.40	0.05
9 THR					0.21	0.22	0.97	0.01
10 GLY					0.28	0.20	0.95	0.02
11 LYS				-0.08		0.24	0.93	-0.01
12 THR					0.70	0.28	0.96	-0.01
13 ILE	1.37	0.46	1.47	-0.20	1.38	0.47	1.76	0.03
14 THR	1.70	0.50		-0.24	1.71	0.53	1.40	-0.01
15 LEU	2.80	0.66		-0.11	2.77	0.71		0.17
16 GLU	4.00	0.88		-0.08	3.98	0.98		0.19
17 VAL	3.91	0.68		0.28	3.82	0.75		0.36
18 GLU	6.23	0.92	2.42	0.91	6.04	1.00		0.73
20 SER	3.46	0.25		0.90	3.28	0.24		0.50
21 ASP	5.73	0.45		1.19	5.45	0.46		
31 GLN		2.88				3.14		
32 ASP					3.40	2.00		
33 LYS	2.28	0.77			2.52	1.23		
34 GLU	1.12	0.82		-1.13	1.30	0.91		
35 GLY				-1.25	-0.09	0.58		
36 ILE		0.71				0.74		
39 ASP						1.12		
40 GLN		1.16				0.86		
41 GLN		1.25				0.98		
42 ARG	-0.81	0.50			-0.80	0.39		
43 LEU	-0.94	0.11			-0.94			
44 ILE	0.40	0.24	3.07	-0.19	0.34	0.17	3.24	
45 PHE			1.86	-0.18	-0.04		2.18	0.26
46 ALA					0.29	0.03	1.55	0.19
47 GLY	0.01	0.02	1.09	-0.12	-0.02	-0.03	1.29	0.13
48 LYS	-0.24	-0.09	1.09	-0.17	-0.30	-0.13	1.38	0.15
49 GLN					-1.18			0.14
50 LEU	-1.07	-0.25			-1.20	-0.37		
55 THR			1.38	0.17		-1.22		0.36
56 LEU		-0.09	3.61	0.72	3.58	-0.16		
57 SER	2.13	-0.12	1.96	0.43	1.94	-0.16	1.73	0.42

58	ASP	0.76	-0.43	1.39	0.19	0.60	-0.49	1.25	0.28
59	TYR	0.62	-0.32	1.49	0.05	0.48	-0.38	1.63	0.30
60	ASN	0.59	-0.19	1.10	0.04	0.49	-0.23	1.16	0.20
61	ILE	1.22	-0.02	1.53	0.06	1.10	-0.05	1.64	0.25
62	GLN	1.26	0.13	1.32	0.08	1.18	0.11	1.44	0.23
63	LYS	1.40	0.19	0.99	0.12	1.34	0.18	1.06	0.18
64	GLU	1.66	0.28	1.14	0.06	1.61	0.29	1.35	0.19
65	SER	1.50	0.23	1.33	0.04	1.44	0.22	1.54	0.21
66	THR	1.06	0.20	1.38	-0.03	1.00	0.18	1.57	0.17
67	LEU	1.52	0.37	2.24	-0.09	1.51	0.36	2.53	0.23
68	HIS	0.81	0.28	2.48	-0.12	0.76	0.23	2.66	0.25
69	LEU	0.70	0.39	2.51	-0.11	0.68	0.36	2.49	0.15
70	VAL	-0.06	0.40	3.23	0.00	-0.09	0.32	2.90	0.24

Table S5. Experimental PCSs (ppm) for **T8-Ln³⁺**-tagged HPPK K76C/C80.

Residue		Tm ³⁺	Yb ³⁺	Residue		Tm ³⁺	Yb ³⁺
2	ILE	-1.01	-0.01	98	ILE	-0.08	0.07
3	GLN	-0.78	0.01	99	LEU	-0.48	0.07
4	ALA	-1.08	0.06	100	LEU	-0.61	0.03
5	TYR	-0.86	0.05	101	TYR	-0.72	-0.03
6	LEU	-0.74	0.15	102	GLY	-0.83	
7	GLY	0.04	0.19	103	GLU	-0.59	-0.03
8	LEU	0.41	0.22	104	GLU	-0.64	-0.05
9	GLY	1.83	0.36	105	MET	-0.54	-0.07
10	SER	1.45	0.23	106	ILE	-0.56	-0.08
11	ASN	2.26	0.26	107	ASP	-0.60	-0.11
12	ILE	2.22	0.24	108	LEU	-0.60	-0.14
13	GLY	1.60	0.14	111	LEU	-0.62	-0.17
15	ARG	0.86	0.08	112	SER	-0.35	-0.07
16	GLU	0.39	0.05	113	VAL	-0.50	
17	SER	0.06	-0.01	115	HIS	-0.21	0.01
18	GLN		0.07	117	ARG	0.21	0.03
19	LEU		0.17	118	MET	0.12	
20	ASN	-0.46	0.09	119	ASN	0.08	0.03
21	ASP		0.02	120	GLU	0.17	0.04
22	ALA		0.29	121	ARG	0.21	0.05
33	SER		0.24	122	ALA	0.27	0.06
34	VAL	-1.81	0.31	123	PHE	0.34	0.08
35	SER	-1.15	0.17	124	VAL	0.28	0.08
36	ASN	-0.94	0.14	125	LEU	0.14	0.07
37	ILE	-0.66	0.10	126	ILE	0.10	0.06
38	SER	-0.45	0.11	128	LEU	-0.04	0.08
40	ILE	-0.14	0.07	129	ASN	-0.10	0.06
41	TYR	0.18	0.10	130	ASP	-0.14	0.06
42	GLU	0.23	0.07	131	ILE	-0.25	0.07
43	THR	0.54	0.09	132	ALA	-0.27	0.05
44	ALA	0.44	0.07	133	ALA	-0.23	0.04
46	VAL	0.76	0.11	134	ASN	-0.24	0.03
47	GLY	0.60	0.08	135	VAL	-0.25	0.03
48	TYR	0.89	0.10	136	VAL	-0.30	0.01
49	THR	0.73	0.08	137	GLU	-0.22	0.01
50	GLU	0.82	0.09	139	ARG	-0.22	-0.01
51	GLN	0.86	0.09	140	SER	-0.14	0.00
53	ASN	0.78	0.09	141	LYS	-0.18	0.00
54	PHE	0.77	0.10	142	LEU	-0.14	0.01
55	LEU	1.00	0.16	143	LYS	-0.14	0.01
56	ASN	0.47	0.12	144	VAL	-0.19	0.02

57	LEU	0.40	0.18	145	LYS	-0.15	0.03
58	CYS	-0.15	0.13	146	ASP	-0.10	0.02
59	VAL	-0.50	0.17	147	LEU	-0.08	0.03
60	GLU	-0.86	0.15	148	VAL	-0.04	0.03
61	ILE	-1.13	0.12	149	PHE	0.05	0.03
62	GLN	-1.34	0.16	150	VAL	0.07	0.03
63	THR	-1.25	0.04	151	ASP	0.12	0.04
65	LEU		-0.11	152	ASP	0.16	0.04
66	THR		-0.42	153	SER	0.24	0.05
67	VAL	-1.94	-0.29	154	VAL	0.21	0.05
68	LEU		-0.46	155	LYS	0.24	0.06
69	GLN		-0.68	156	ARG	0.05	0.04
95	ASP	3.37	0.50	157	TYR	0.05	0.05
96	VAL	3.66	0.57	158	LYS	-0.03	0.04
97	ASP	0.86	0.27				

Table S6. Experimental PCSs (ppm) for T7-Tm³⁺-tagged HPPK K76C/C80

Residue		PCS	Residue		PCS
2	ILE	0.22	134	ASN	0.54
3	GLN	0.57	135	VAL	0.59
4	ALA	1.35	136	VAL	0.50
38	SER	1.54	137	GLU	0.50
42	GLU	0.68	139	ARG	0.48
48	TYR	0.71	140	SER	0.45
50	GLU	0.43	141	LYS	0.39
51	GLN	0.48	142	LEU	0.41
63	THR	0.73	143	LYS	0.38
101	TYR	0.95	145	LYS	0.52
103	GLU	0.39	146	ASP	0.45
104	GLU	0.46	147	LEU	0.48
106	ILE	0.44	149	PHE	0.54
110	LYS	-0.06	150	VAL	0.40
111	LEU	0.32	151	ASP	0.48
119	ASN	0.79	153	SER	0.47
122	ALA	0.75	154	VAL	0.53
129	ASN	0.86	158	LYS	0.55

Table S8. Experimental ${}^1D_{\text{HN}}$ RDCs of **T8-Tm³⁺**-tagged ubiquitin E24C/A28C and HPPK K76C/C80, measured at 600 MHz.

Ubiquitin E24C/A28C			HPPK K76C/C80			HPPK K76C/C80		
Residue	${}^1D_{\text{HN}}$ RDC (Hz)		Residue	${}^1D_{\text{HN}}$ RDC (Hz)		Residue	${}^1D_{\text{HN}}$ RDC (Hz)	
2	GLN	10.7	3	GLN	-15.3	105	MET	-1.3
3	ILE	8.2	4	ALA	-5.7	108	LEU	-15.0
4	PHE	-10.0	5	TYR	-12.9	111	LEU	-17.8
6	LYS	-17.0	6	LEU	-7.4	113	VAL	-16.3
7	THR	-12.6	16	GLU	-0.3	118	MET	3.9
16	GLU	10.0	17	SER	12.7	119	ASN	-13.7
18	GLU	4.7	20	ASN	5.2	120	GLU	-2.4
33	LYS	-12.9	34	VAL	-7.4	121	ARG	16.5
34	GLU	0.4	36	ASN	-9.4	122	ALA	28.6
36	ILE	-2.7	38	SER	-11.8	124	VAL	11.3
44	ILE	-14.5	40	ILE	-16.7	125	LEU	20.2
45	PHE	-15.1	41	TYR	-8.3	126	ILE	12.3
48	LYS	-9.9	42	GLU	-7.4	128	LEU	18.8
55	THR	-12.9	44	ALA	-13.6	129	ASN	24.6
56	LEU	-5.3	51	GLN	-10.9	130	ASP	4.3
57	SER	5.4	53	ASN	-8.2	131	ILE	5.2
58	ASP	4.4	54	PHE	-3.3	133	ALA	-14.5
61	ILE	16.3	56	ASN	-9.2	134	ASN	2.2
62	GLN	8.0	57	LEU	-14.4	135	VAL	-5.4
65	SER	10.7	58	CYS	-12.0	136	VAL	28.2
66	THR	-4.1	59	VAL	-11.8	137	GLU	4.6
68	HIS	-15.9	60	GLU	-15.0	140	SER	-14.7
69	LEU	-4.6	61	ILE	-11.6	141	LYS	-7.2
70	VAL	6.7	62	GLN	-13.4	142	LEU	-5.7
			63	THR	-9.2	144	VAL	26.7
			67	VAL	-15.0	145	LYS	28.9
			95	ASP	-7.7	146	ASP	10.5
			98	ILE	-5.7	148	VAL	22.1
			100	LEU	-8.7	149	PHE	-5.6
			101	TYR	-7.4	151	ASP	8.5
			102	GLY	-20.0	153	SER	-17.8
			103	GLU	18.6	155	LYS	-7.0
			104	GLU	-11.7	158	LYS	-6.7

References

1. M. D. Lee, M. L. Dennis, J. D. Swarbrick and B. Graham, *Chem. Commun.* **2016**, 52, 7954–7957.
2. M. D. Lee, C. Loh, J. Shin, S. Chhabra, M. L. Dennis, G. Otting, J. D. Swarbrick and B. Graham, *Chem. Sci.* **2015**, 6, 2614–2624.
3. H. E. Gottlieb, V. Kotlyar and A. Nudelman, *J. Org. Chem.* **1997**, 62, 7512–7515.
4. J. D. Swarbrick, P. Ung, X. Su, A. Maleckis, S. Chhabra, T. Huber, G. Otting and B. Graham, *Chem. Commun.* **2011**, 47, 7368–7370.
5. S. Chhabra, O. Dolezal, B. M. Collins, J. Newman, J. S. Simpson, I. G. Macreadie, R. Fernley, T. S. Peat and J. D. Swarbrick, *PLoS One*, **2012**, 7, e29444.
6. F. Delaglio, S. Grzesiek, G. W. Vuister, G. Zhu, J. Pfeifer and A. Bax, *J. Biomol. NMR*, **1995**, 6, 277–293.
7. T.D. Goddard and D. G. Kneller, SPARKY 3, University of California, San Francisco
8. C. Schmitz, M. J. Stanton-Cook, X.-C. Su, G. Otting and T. Huber, *J. Biomol. NMR*, **2008**, 41, 179–189.
9. A. S. Maltsev, A. Grishaev, J. Roche, M. Zasloff and A. Bax, *J. Am. Chem. Soc.* **2014**, 136, 3752–3755.
10. M. Zweckstetter, *Nat. Protoc.* **2008**, 3, 679–690.